

Passage Times for Polymer Translocation Pulled through a Narrow Pore

Debabrata Panja

Institute for Theoretical Physics, Universiteit van Amsterdam, Valckenierstraat 65, 1018 XE Amsterdam, The Netherlands

Gerard T. Barkema^{†‡}

[†]*Institute for Theoretical Physics, Universiteit Utrecht, Leuvenlaan 4, 3584 CE Utrecht, The Netherlands*

[‡]*Instituut-Lorentz, Universiteit Leiden, Niels Bohrweg 2, 2333 CA Leiden, The Netherlands*

We study the passage times of a translocating polymer of length N in three dimensions, while it is pulled through a narrow pore with a constant force F applied to one end of the polymer. At small to moderate forces, satisfying the condition $FN^\nu/k_BT \lesssim 1$, where $\nu \approx 0.588$ is the Flory exponent for the polymer, we find that τ_N , the mean time the polymer takes to leave the pore, scales as $N^{2+\nu}$ independent of F , in agreement with our earlier result for $F = 0$. At strong forces, i.e., for $FN^\nu/k_BT \gg 1$, the behaviour of the passage time crosses over to $\tau_N \sim N^2/F$. We show here that these behaviours stem from the polymer dynamics at the immediate vicinity of the pore — in particular, the memory effects in the polymer chain tension imbalance across the pore.

I. INTRODUCTION

Molecular transport through cell membranes is an essential mechanism in living organisms. Often, the molecules are too long, and the pores in the membranes too narrow, to allow the molecules to pass through as a single unit. In such circumstances, the molecules have to deform themselves in order to squeeze — i.e., translocate — themselves through the pores. DNA, RNA and proteins are such naturally occurring long molecules (1; 2; 3; 4; 5) in a variety of biological processes. Translocation is also used in gene therapy (6; 7), in delivery of drug molecules to their activation sites (9), and as a potentially cheaper alternative for single-molecule DNA or RNA sequencing (8; 16). Consequently, the study of translocation is an active field of research: as a cornerstone of many biological processes, and also due to its relevance for practical applications.

Translocation in living organisms is a complex process. Take for instance the case of gene expression: most proteins are synthesized within the cytoplasm. Their subsequent accurate and swift delivery to target sites, requiring energy, is a crucial step in gene expression. In different situations the energy is provided by chaperon molecules (11), pH gradient (12) or molecular motors across membranes (13). These delivery mechanisms can be further complicated by membrane fluctuations and sometimes by gates that control the accessibility of the pores (14). In view of such complexity, translocation as a biological or biophysical process in living organisms has been scrutinized in a variety of *in vivo* experimental situations [see e.g. Ref. (15) and the references therein].

The experimental developments have been followed by a number of mean-field type theoretical studies on polymer translocation (20).

More recently, translocation has found itself at the forefront of single-molecule-detection experiments (8; 17), as new developments in design and fabrication of nanometer-sized pores and etching methods may lead to

cheaper and faster technology for the analysis and detection of single macromolecules. The underlying principle for these experiments is that of a Coulter counter: molecules suspended in an electrolyte solution pass through a narrow pore in a membrane. The electrical impedance of the pore increases with the entrance of a molecule as it displaces its own volume of the electrolyte solution. By applying a voltage over the pore, the passing molecules are detected as current dips. For nanometer-sized pores (slightly larger than the molecule's cross-section) the magnitude and the duration of these dips have proved to be effective in determining the size and length of the molecules. In the case of DNA sequencing at nucleotide level, usage of protein pores (modified α -haemolysin, mitochondrial ion channel, nucleic acid binding/channel protein etc.), and etching specific DNA sequences inside the pores (6; 18) have opened up promising new avenues of fast, simple and cheap technology for single macromolecule detection, analysis and characterization [see Ref. (19) for a recent development].

The subject of this paper is a translocating polymer threaded through a narrow pore in an immobile membrane, where a bead is attached to one end of the polymer, and the bead is pulled by an optical tweezer with a constant force. Such a setup can be used to spread apart a partially unzipped dsDNA molecule — of which one strand is threaded through the pore — a process that can quantify the forces involved in basepair unzipping kinetics (21). In theoretical literature, this problem has been considered in recent times: for polymer length N and applied force F , in Ref. (22), in the *absence* of hydrodynamical interactions, a lower bound $\propto N^2$ for small forces ($FN^\nu/k_BT \leq 1$) has been argued for the polymer's mean unthreading time τ_N , the average time it takes for the polymer to leave the pore. The lower bound holds in the limit of unimpeded polymer movement, i.e., for an infinite pore, or equivalently, in the absence of the membrane. Simulation data (in two-dimensions) presented in Ref. (22) indicated that the lower bound may very well

be valid in the limit of narrow pores as well. The same problem, also in the *absence* of hydrodynamical interactions, has been numerically studied in two-dimensions in Ref. (23). It reported that for narrow pores $\tau_N \sim N^2$ with the velocity of translocation $v(t) \sim N^{-1}$ for moderate and strong forces. As the force-dependence of τ_N is concerned, Ref. (23) reported numerical results that in the absence of the membrane $\tau_N \sim F^{-2+\frac{1}{\nu}}$ for moderate forces, and $\tau_N \sim F^{-1}$ for strong forces, while for narrow pores $\tau_N \sim F^{-1}$ for moderate to strong forces.

The purpose of this paper is to revisit the problem of translocation of a polymer pulled through a narrow pore in the *absence* of hydrodynamical interactions, in order to provide a deeper theoretical understanding of the polymer dynamics under these conditions, as well as of the scaling behaviour of the unthreading time of the polymer. In support of our theory, we perform high precision computer simulations, using a *three-dimensional self-avoiding lattice polymer model* that we have used before to study polymer translocation (24; 26; 27) and several other situations (28). Our conventions to study this problem, all throughout this paper, is the following. We place the membrane at $z = 0$, and thread the polymer of *total length* $2N$ halfway through the pore such that both the right ($z > 0$) and the left ($z < 0$) of the membrane have equal number of monomers N . We fix the middle monomer (monomer number N) at the pore, apply a force F on the free end on the right and let both left and right segments of the polymer come to equilibrium. At $t = 0$ we release the middle monomer and let translocation commence. The mean time τ_N that the polymer remains within the pore is defined as the mean unthreading time for polymer length N under the force F . Additionally, we use $k_B T = 1$, although $k_B T$ is explicitly mentioned at several places in the paper.

Our main results in this paper are as follows. At small to moderate forces, satisfying the condition $FN^\nu \lesssim 1$, where $\nu \approx 0.588$ is the Flory exponent for the polymer, we find that τ_N is independent of F . In agreement with our earlier result for unbiased polymer translocation; i.e., for $F = 0$ (24), τ_N scales with polymer length as $\tau_N \sim N^{2+\nu}$. At strong forces, i.e., for $FN^\nu \gg 1$, we find $\tau_N \sim N^2/F$. While these results agree with the existing ones (22; 23) in broad terms, we show that $v(t)$, the velocity of translocation is *not* constant in time. In fact, for strong forces, we show that the velocity of translocation $v(t)$ behaves as $t^{-1/2}$, while for small to moderate forces the behaviour of $v(t)$ is more complicated. The physical picture provided in Refs. (22; 23), wherein the scaling arguments for the unthreading time involved a constant velocity of translocation (albeit an average one, in light of this work) is incomplete (29). Using theoretical analysis supported by high-precision simulation data, we show that these behaviours stem from the dynamics of the polymer segments at the immediate vicinity of the pore — in particular, the memory effects in the polymer chain tension imbalance across the pore. The theoretical analysis presented here is based on that of Ref. (24), and

therefore provides a direct confirmation of the robustness of the theoretical method presented in Ref. (24).

This paper is organized in the following manner. In Sec. II we discuss a method to measure component of the polymer chain tension which is perpendicular to the membrane. In Sec. III we analyze the memory effects in $\phi(t)$, the imbalance of this component of the polymer chain tension. In Sec. IV we discuss the consequence of these memory effects on the translocation velocity $v(t)$, and obtain the relation between the mean unthreading time τ_N and the polymer length N . We finally end this paper with a discussion in Sec. V.

II. CHAIN TENSION PERPENDICULAR TO THE MEMBRANE

A translocating polymer should be thought of as two segments of polymers threaded at the pore, while the segments are able to exchange monomers between them through the pore. In Ref. (24) we developed a theoretical method to relate the dynamics of translocation to the imbalance of chain tension between these two segments across the pore. The key idea behind this method is that the exchange of monomers across the pore responds to $\phi(t)$, this imbalance of chain tension; in its turn, $\phi(t)$ adjusts to $v(t)$, the transport velocity of monomers across the pore. Here, $v(t) = \dot{s}(t)$ is the rate of exchange of monomers from one side to the other, where $s(t)$ is the total number of monomers transferred from one side of the pore to the other in time $[0, t]$. In fact, we noted that $s(t)$ and $\phi(t)$ are conjugate variables in the thermodynamic sense, with $\phi(t)$ playing the role of the chemical potential difference across the pore.

By definition, $\phi(t) = \Phi_R(t) - \Phi_L(t)$ where $\Phi_R(t)$ and $\Phi_L(t)$ are respectively the chain tension (or the chemical potential) on the right and the left side of the pore. Consider a separate problem, where we tether one end of a polymer to a fixed membrane, yet the number of monomers are allowed to spontaneously enter or leave the tethered end, then we have

$$\frac{W_t(- \rightarrow +)}{W_t(+ \rightarrow -)} = \exp[\Phi(t)/k_B T], \quad (1)$$

where $W_t(- \rightarrow +)$ [resp. $W_t(+ \rightarrow -)$] is the rate that a monomer enters (resp. leaves) the polymer chain through the tethered end at time t . Note that tethering the polymer while allowing monomers to enter or leave the polymer at the tethered end is precisely the case that translocation represents.

Returning to our problem of a translocating polymer under a pulling force F , note that at $t = 0$, when the left and the right segments are equilibrated with $F = 0$ and $F \neq 0$ respectively, it is easy to use Eq. (1) to measure the chain tension for both segments at the pore [$\Phi(t = 0)$ in our notation], since under these conditions, we also have the relation that

$$P_- W_{t=0}(- \rightarrow +) = P_+ W_{t=0}(+ \rightarrow -), \quad (2)$$

where P_- (resp. P_+) is the probability that the (left or the right) polymer segment has one monomer less (resp. one extra monomer). Equations (1) and (2) together yield us

$$\Phi(t=0) = k_B T \ln \frac{P_+}{P_-}. \quad (3)$$

Note that even for $F = 0$, there is nonzero chain tension, due to the presence of the membrane. A polymer's free energy close to a membrane is higher than its free energy in bulk. In other words, the membrane repels the polymer, and as a result, for a polymer with one end tethered to a membrane, the monomers close to the membrane are more stretched than they would be in the bulk.

The chain tension as obtained from Eq. (3) is linearly related to the z -coordinate of the centre-of-mass of the first few monomers along the polymer's backbone, at the immediate vicinity of the pore, at least for the relatively modest forces used in our simulations. This is shown in Fig. 1, where for a tethered polymer of length $N = 100$, the average distance $\langle Z^{(4)}(t=0) \rangle$ of the centre-of-mass of the first 4 monomers along the polymer's backbone, counting from the tethered end of a polymer, is plotted versus the chain tension Φ , while its free end is pulled with various force strengths F . Within the error bars, all the points in Fig. 1 fall on a straight line, implying that Φ is very well-proxied by $\langle Z^{(4)} \rangle$. Note in Fig. 1 that the black line does not pass through the origin, which shows that $\Phi_{F=0} \neq 0$, as we argued above. Since measurements of the chain tension via Eq. (3) are much more noisy than measurements of $\langle Z^{(4)} \rangle$, we will use the latter quantity as a measure for the chain tension.

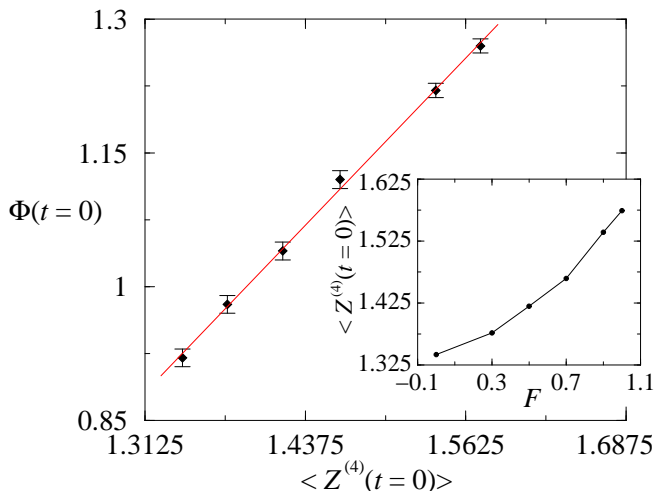


FIG. 1 $\langle Z^{(4)}(t=0) \rangle$ vs. $\Phi(t=0)$ demonstrating the linear relationship between the two, for $N = 100$ and $F = 0.0, 0.3, 0.5, 0.7, 0.9$ and 1.0 respectively. The angular brackets for $\langle Z^{(4)}(t=0) \rangle$ indicates an average over 12,800,000 polymer realizations. The data for $\Phi(t=0)$ are obtained 2,400 polymer realizations. The red line corresponds to the linear best-fit. Inset: $\langle Z^{(4)}(t=0) \rangle$ as a function of F .

III. MEMORY EFFECTS IN THE z -COMPONENT OF THE CHAIN TENSION

In the case of unbiased polymer translocation, we have witnessed in Ref. (24) that the memory effects of the polymer gives rise to anomalous dynamics of translocation. We argued (24) that the imbalance of the chain tension $\phi(t)$ across the pore and the number of monomers $s(t)$ that have crossed from one side of the membrane to the other in time $[0, t]$ are conjugate variables in the thermodynamic sense. Additionally, $\phi(t)$ is related to the translocation velocity $v(t)$ by the relation $\phi(t) = \phi_{t=0} - \int_0^t dt' \mu(t-t')v(t')$ via the memory kernel $\mu(t)$, which can be thought of as the ‘impedance’ of the system. On average, there will not be an imbalance in chain tension if no force is applied, but there will be fluctuations in chain tension. When the polymer is pulled by a force F to the right, the symmetry between the polymer segments on two sides of the membrane (viz., the polymer segments on the right are more stretched than those on the left of the membrane), are destroyed. As a result, on average $\phi(t)$, $\phi_{t=0}$ and $v(t)$ are non-zero, and from now on, we understand these three quantities as an average over all the unthreading polymers. Additionally, for $F \neq 0$ the memory effects continue to be present, and the memory kernels $\mu_L(t)$ and $\mu_R(t)$ for the polymer segments on the left and the right sides of the membrane are different. In Ref. (24) we determined $\mu_L(t) \equiv \mu_{F=0}(t)$ by tethering a polymer of length $N - 10$ on a fixed membrane, where we injected p monomers at the tethered end at time $t = 0$, i.e., $v(t) = p\delta(t)$ with $p = 10$ (bringing the final polymer length to N), and proxying $\phi(t)$ by the average distance of the centre-of-mass of the first 5 monomers $\langle Z^{(5)}(t) \rangle$ from the membrane. We found

$$\mu_L(t) \sim t^{-\frac{1+\nu}{1+2\nu}} \exp(-t/\tau_{\text{Rouse}}), \quad (4)$$

where $\tau_{\text{Rouse}} \sim N^{1+2\nu}$ is the Rouse time, the longest relaxation time-scale of a polymer of length N .

Following the same line as presented in Ref. (24), here we compute $\mu_R(t)$, the memory effect of a polymer of length N with one end tethered to a membrane, and the other end pulled by a force F . The first step to do this is to obtain the relaxation time for a polymer of length N under these conditions. For $F = 0$ the result for the relaxation time $\sim \tau_{\text{Rouse}}$ is well-known [and has been confirmed in an earlier study of ours (27)], but with $F \neq 0$, to the best of our knowledge, the corresponding analytical result does not exist. We therefore resort to simulations: we denote the vector distance of the free end of the polymer w.r.t. the tethered end at time t by $\mathbf{e}(t)$, and define the correlation coefficient for the end-to-end vector as

$$c(t) = \frac{\langle \mathbf{e}(t) \cdot \mathbf{e}(0) \rangle - \langle \mathbf{e}(t) \rangle \cdot \langle \mathbf{e}(0) \rangle}{\sqrt{\langle \mathbf{e}^2(t) \rangle - \langle \mathbf{e}(t) \rangle^2} \sqrt{\langle \mathbf{e}^2(0) \rangle - \langle \mathbf{e}(0) \rangle^2}}. \quad (5)$$

The angular brackets in Eq. (5) denote simple ensemble averaging for $F \neq 0$. We first obtain the time correlation coefficients $c(t)$ for 256 independent polymers, and $\bar{c}(t)$

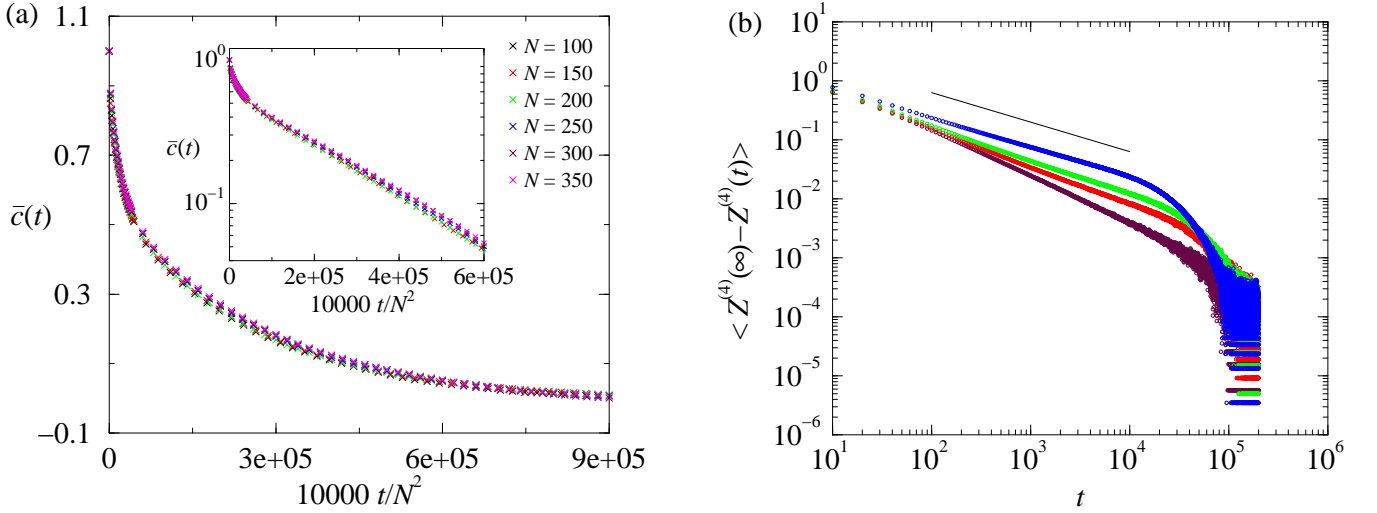


FIG. 2 (a) $\bar{c}(t) \sim \exp(-t/\tau_F)$ for strong forces, with $\tau_F \sim N^2$; the data shown correspond to $F = 1.0$; data obtained using 256 polymers for each value of N . Inset: the same data are shown in semi-log plot to show that the decay of $\bar{c}(t)$ in time is exponential at long times. (b) Behaviour of $\mu_R(t)$, proxied by $\langle Z^{(4)}(t) \rangle$, for $N = 100$ and four different values of F : $F = 0.0$ (maroon), $F = 0.3$ (red), $F = 0.5$ (green), and $F = 1.0$ (blue); the solid black line corresponds to a slope $t^{-1/2}$; data obtained using 12, 800, 000 polymers for each value of F . See text for more details.

is a further arithmetic mean of the corresponding 256 different time correlation coefficients. At strong forces, when we scale the units of time by factors of N^2 (for self-avoiding polymers!), the $\bar{c}(t)$ vs. t curves collapse on top of each other. This is shown in Fig. 2(a) for $F = 1.0$ and $N = 100, \dots, 350$.

What happens at small to moderate forces to the relaxation time is not entirely clear to us. We do not expect the relaxation time-scale to change continuously with F . Thus, given the two limits $\tau_{\text{Rouse}} \sim N^{1+2\nu}$ for $F = 0$ and $\tau_F \sim N^2$ for strong forces, we believe that at small to moderate forces the relaxation time becomes a linear combination of $\tau_{\text{Rouse}} \sim N^{1+2\nu}$ and $\tau_F \sim N^2$, with the coefficients of these two times varying with the magnitude of F .

While Fig. 2(a) provides the answer to the relaxation of the *entire* polymer for strong forces, the second step to identify α for $\mu_R(t) \sim t^{-\alpha} \exp(-t/\tau_F)$ for some α for strong forces is to analyze the relaxation of the polymer segments at the immediate vicinity of the tethered point. The value of α depends on the relaxation properties following the event of injecting, say, p extra monomers at the tether end, just like extra monomers add to (or get taken out of) the right segment of the polymer during translocation. Given the $\exp(-t/\tau_F)$ behaviour of Fig. 2(a), we anticipate that by time t after the extra monomers are injected at the tethered point, the extra monomers will come to a steady state across the inner part of the polymer up to $n_t \sim t^{1/2}$ monomers from the tethered point, but not significantly further. This internal section of $n_t + p$ monomers in steady state extends only to $r(n_t)$ from the membrane, because the larger scale conformation has yet to adjust, and consequently there

is a compressive force f on these n_t monomers.

For $F = 0$, $r(n_t) \sim n_t^\nu$ is the only length scale for the equilibrated section of the chain, which leads to $f_{F=0} \sim k_B T \delta r / r^2$ (24), but for $F \neq 0$ this does not hold. For small to moderate forces, i.e., for $FN^\nu / k_B T \lesssim 1$, the polymer conformation is given by a sequence of blobs of size ξ , given by the relation $F\xi = k_B T$ and for strong forces, i.e., for $FN^\nu / k_B T \gg 1$, $\xi \rightarrow a$, where a is the size of a single monomer (22; 25). Thus, for $F \neq 0$, the shape of the polymer resembles that of a cylinder, implying $f_{F \neq 0} \sim k_B T \delta r / (r\xi)$. The independence of ξ on n_t implies that $r(n_t) \sim n_t$, which allows us to write $f_{F \neq 0} \sim k_B T \delta n_t / (n_t \xi) \sim t^{-1/2}$. This force is transmitted to the membrane, through a combination of decreased tension at the tether and increased incidence of other membrane contacts. The fraction borne by reducing tension leads us to what is, strictly speaking, an inequality: $\alpha \geq 1/2$. However, it seems unlikely that the adjustment at the membrane should be disproportionately distributed between the two nearly balancing effects of polymer chain tension and monomeric repulsion, leading to the expectation that the inequality becomes an equality.

Theoretically however, we cannot rule out the larger values for α , but our numerical results in Fig. 2(b), where we have used $\langle Z^{(4)}(t) \rangle$ to proxy $\Phi_R(t)$ and $p = 5$, for strong forces favour the smallest theoretical value, namely $\alpha = 1/2$. The power law decay preceding the exponential ones in Fig. 2(b) change from $t^{-\frac{1+\nu}{1+2\nu}}$ at $F = 0$ to $t^{-1/2}$ for strong forces ($FN^\nu / k_B T \gg 1$). Following the discussion about relaxation times for small to moderate forces three paragraphs above, we believe that between $F = 0$ and $FN^\nu / k_B T \gg 1$ the decay for $\Phi_R(t)$ at short

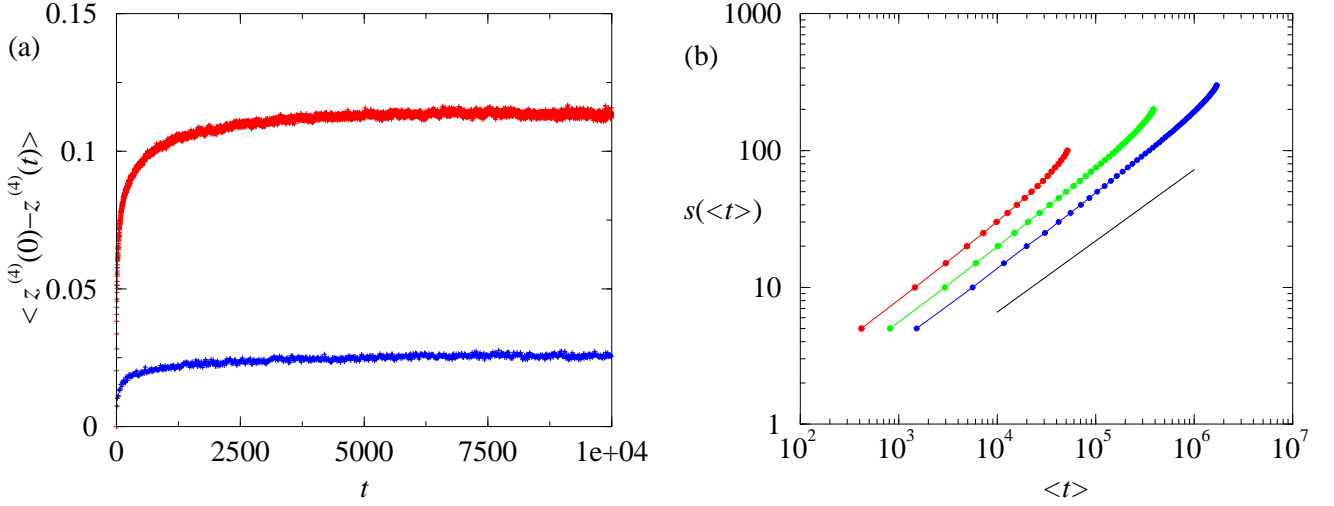


FIG. 3 (a) Behaviour of $\phi(0) - \phi(t)$ for $N = 100$ as a function of t , shown by means of the proxy variable $\langle z^{(4)}(0) - z^{(4)}(t) \rangle$, showing that $\phi(0) - \phi(t)$ reduces to a constant very quickly: $F = 1.0$ (red) and $F = 0.5$ (blue). The angular brackets denote an average over 672,000 polymer realizations. (b) Mean time required, for $F = 1.0$, to unthread a distance s for $s = 5, 10, 15, \dots, N$: $N = 100$ (red), $N = 200$ (green), $N = 300$ (blue). The time-axis corresponding to $N = 200$ is the true time, for the $N = 100$ and $N = 300$ cases the time axis is divided and multiplied by a factor 2 respectively. This is done in order to show that the slope of the curves reduces slowly with increasing N : we obtain, for $N = 100$ a slope of 0.57, for $N = 200$ a slope of 0.54, and $N = 300$ a slope of 0.52 at short times. At long times the slope increases for all values of N : most likely due to the fact that the monomer at the pore is too close to the end of the polymer. The solid black line correspond to a slope of 0.52. The angular brackets denote an average over 48,000 polymer realizations. See text for more details.

times is a combination of these two power laws. Additionally, closer inspection of the curves for $F = 0.3$ and $F = 0.5$ in Fig. 2(b) reveals that the slope is steeper in the beginning: perhaps it is an indication that relaxation within a blob (corresponding to $t^{-\frac{1+\nu}{1+2\nu}}$) precedes inter-blob rearrangements (corresponding to $t^{-1/2}$). Nevertheless, at strong forces, the behaviour

$$\mu_R(t) \sim t^{-\frac{1}{2}} \exp(-t/\tau_F), \quad \text{with } \tau_F \sim N^2, \quad (6)$$

stands as a witness of the fact that the Flory-like structure of the polymer is entirely destroyed.

IV. THE RELATION BETWEEN $\phi(t)$ AND $v(t)$, AND THE SCALING BEHAVIOUR OF τ_N

A. Relation between the imbalance of chain tension $\phi(t)$ and the translocation velocity $v(t)$

In this subsection we consider the strong force case as it is simpler. The moderate to weak force case is discussed in Sec. IV.B.

So far, we have $\mu_L(t) \sim t^{-\frac{1+\nu}{1+2\nu}} \exp(-t/\tau_{\text{Rouse}})$ and $\mu_R(t) \sim t^{-1/2} \exp(-t/\tau_F)$ for strong forces. Since the memory effects in the dynamics of the translocating polymer stem from the power laws, in the absence of symmetry between the left and the right segment of the polymer, we only need to keep track of the power law of $\mu_R(t)$, as it has a *lower* exponent than $\mu_L(t)$. In other words, in

the relation

$$\phi(t) = \phi_{t=0} - \int_0^t dt' |\mu(t-t')| v(t'), \quad (7)$$

we have to use the fact that the power law decay of $\mu(t)$ behaves $\sim t^{-1/2}$. Note the absolute value around $\mu(t)$, as the sign of $\mu(t)$ is negative.

Equation (7) can be inverted via Laplace transformation, yielding

$$v(k) = \frac{\phi_{t=0}}{k|\mu(k)|} - \frac{\phi(k)}{|\mu(k)|}, \quad (8)$$

where k is the Laplace variable representing inverse time. Thereafter, using $\mu(t) \sim t^{-1/2}$, i.e., $\mu(k) \sim k^{-1/2}$, and Laplace-inverting Eq. (8), we get

$$v(t) = \int_0^t dt' (t-t')^{-3/2} [\phi_{t=0} - \phi(t')]. \quad (9)$$

B. Scaling behaviour of τ_N with N

In Eq. (9), if $\phi(t)$ goes to a constant $\neq \phi_{t=0}$, then

$$v(t) \sim t^{-1/2} \quad \text{i.e.,} \quad s(t) = \int_0^t dt' v(t') \sim t^{1/2}, \quad (10)$$

where $s(t)$ is the distance unthreaded in time t (30).

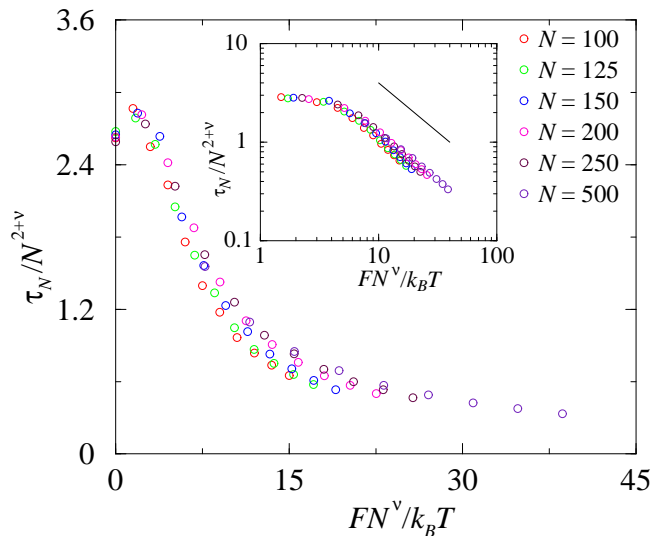


FIG. 4 Collapse of all data in terms of $FN^\nu/k_B T$ and $\tau_N/N^{2+\nu}$ for $F = 0.0, 0.1, 0.2, \dots, 1.0$. Inset: the same data in log-log plot, the black line corresponds to a slope of -1 . The τ_N values correspond to the median for 1,024 polymer unthreading events.

In Fig. 3(a) we show the behaviour of $[\phi_{t=0} - \phi(t)]$ by means of the proxy variable $\langle z^{(4)}(0) - z^{(4)}(t) \rangle$ for strong forces [$F = 1.0$ (red) and $F = 0.5$ (blue)], where $z^{(4)}(t)$ is the difference between the $Z^{(4)}(t)$ values between the right and left segment of the polymer, i.e., $z^{(4)}(t) = Z_R^{(4)}(t) - Z_L^{(4)}(t)$. Indeed $[\phi_{t=0} - \phi(t)]$ goes to a constant fairly quickly. Following Eq. (10), this yields us the scaling $s(t) \sim t^{1/2}$ for strong forces. The data in support of the scaling $s(t) \sim t^{1/2}$ are shown in Fig. 3(b), for $F = 1.0$.

The scaling for the mean unthreading time τ_N is obtained from the equation $s(\tau_N) = N$. For strong forces, it is derivable as $\tau_N \sim N^2$ — as shown in Fig. 4(a) or in earlier works (22; 23) — from Eq. (10) if we assume that $[\phi_{t=0} - \phi(t)]$ is a constant *independent* of N . It seems reasonable (and likely!) that a local property like $[\phi_{t=0} - \phi(t)]$ should be unaffected by the polymer length, which is a large-scale property; nevertheless, we have no way to argue this theoretically. In the context of using Eq. (10) to obtain $\tau_N \sim N^2$, it is however useful to note that in the scaling sense τ_N is smaller than (or equal to) the time scales in the exponential decay of $\mu_R(t)$ and $\mu_L(t)$, otherwise the power-law behaviour of $\mu(t)$ we used in Eq. (710) would not have been applicable for all times $t < \tau_N$.

The collapse of all the data for the unthreading times for several different values of N and F in terms of the variables $FN^\nu/k_B T$ and $\tau_N/N^{2+\nu}$, as shown in Fig. 4, indicates that the unthreading time τ_N can be written in a scaling form as

$$\tau_N \sim N^{2+\nu} g\left(\frac{FN^\nu}{k_B T}\right), \quad (11)$$

where $g(x)$ is a scaling function of its argument x . Figure 4 shows that $g(x) \sim 1/x$ for $x \gg 1$. Note that $g(0)$ is a constant, in agreement with our earlier result that the unthreading time scales as $N^{2+\nu}$ in for unbiased translocation (24), in which case the polymer leaves the pore purely due to thermal fluctuations.

The fact that $g(0)$ is a constant indicates that $g(x)$ has to deviate from the $1/x$ behaviour as x approaches zero. From the inset of Fig. 4 we see that $g(x)$ starts to deviate from the $1/x$ behaviour at about $x = 4$, at which point the force is moderate in strength. In Fig. 4, note also that $\tau_N/N^{2+\nu}$ has a higher prefactor close to $x = 0$ than at $x = 0$.

A priori, the same analysis (7-10) holds for small to moderate forces as well. Nevertheless, whether Eq. (9) is actually useful in such circumstances is a different matter. Indeed, a deeper investigation reveals that $\phi_{t=0}$ for small to moderate forces can be extremely small. To give a feeling for how small $\phi_{t=0}$ can be, we obtained $\langle Z^{(4)}(t=0) \rangle$ values for $N = 100$ for $F = 0.0, 0.1, \dots, 1.0$ (not all are plotted in Fig. 1). The $\langle Z^{(4)}(t=0) \rangle$ values for $F = 0.1, \dots, 0.3$ (approximate x -values 1.5, 3 and 4.5 in Fig. 4), corresponding to the right segment of the polymer, turned out to be 1.35, 1.36 and 1.38 respectively, while $\langle Z^{(4)}(t=0) \rangle$ corresponding to $F = 0.0$ (i.e., for the left segment of the polymer) turned out to be 1.34.

Since $FN^\nu/k_B T$ is a dimensionless parameter that describes the effect of the force on the polymer's dynamics compared to the effect of thermal fluctuations, it seems logical that if $FN^\nu/k_B T$ is slowly reduced, thermal fluctuations start to dominate over the effect of the force, and translocation by the pulling force F starts to resemble unbiased translocation, i.e., translocation in the absence of any external forces (24; 26; 27). Such a picture is manifested by both sides of Eq. (9) effectively becoming zero as suggested in the above paragraph; the equation remains valid, but ceases to be useful in practice.

V. DISCUSSION

In this paper, we have considered polymer translocation pulled through a narrow pore by a force F . We have provided a theoretical description of the polymer's dynamics under these conditions, as well as of the scaling behaviour of the unthreading time τ_N for the polymer of total length $2N$, the time the polymer takes to leave the pore. Our theory is supported by high precision computer simulation data, generated for a three-dimensional self-avoiding lattice polymer model.

At strong forces, i.e., for $FN^\nu \gg 1$, we have reported $\tau_N \sim N^2/F$: we have shown that the translocation velocity $v(t)$ is *not* constant in time; in fact, the velocity of translocation $v(t)$ is shown to behave as $t^{-1/2}$, while for small to moderate forces the behaviour of $v(t)$ is more complicated. At small to moderate forces, satisfying the condition $FN^\nu \lesssim 1$, where $\nu \approx 0.588$ is the Flory exponent for the polymer, we have found that τ_N is indepen-

dent of F , and in agreement with our earlier result for unbiased polymer translocation (24) scales with polymer length as $\tau_N \sim N^{2+\nu}$.

We have shown that the scaling of $v(t)$ as well as the N -dependent part of τ_N stem from the dynamics of the polymer segments at the immediate vicinity of the pore — in particular, the memory effects in the polymer chain tension imbalance across the pore. The theoretical analysis presented here is based on that of Ref. (24), and therefore provides a direct confirmation of the robustness of the theoretical method presented in Ref. (24). Additionally, we note that the physical picture provided in Refs. (22; 23), wherein the scaling arguments for the unthreading time involved a constant velocity of translocation (albeit an average one, in light of this work) is incomplete.

It should nevertheless be mentioned that the dependence of the relevant quantities, such as $v(t)$ or τ_N on F is beyond the scope of the theoretical description provided here. The main reason behind this is that no analytical expression has been reported (neither do we have one ourselves) for the quantities, such as the polymer chain tension, memory kernel etc. for force F . Indeed, the behaviour of the quantities of interest on F is complicated, as already manifested by Fig. 1, and in the absence of a theoretical description involving F , numerical investigation has remained the only way. Nevertheless, we note that the y -axis of Fig. 4 as $\tau_N/N^{2+\nu}$ [originating from our previous work (24)], the x -axis of Fig. 4 as $FN^\nu/k_B T$ as a measure of the strength of the force in relation to thermal fluctuations, and the scaling $\tau_N \sim N^2$ at strong forces automatically imply that τ_N has to behave $\sim 1/F$ at strong forces.

Acknowledgements: We gratefully acknowledge our discussions with Prof. Robin C. Ball. Virtually unlimited computer time from the Dutch National supercomputer cluster SARA is also acknowledged.

References

- [1] B. Dreiseikelmann, *Microbiol. Rev.* **58**, 293 (1994).
- [2] J. P. Henry *et al.*, *J. Membr. Biol.* **112**, 139 (1989).
- [3] J. Akimaru *et al.*, *PNAS USA* **88**, 6545 (1991).
- [4] D. Goerlich and T. A. Rappaport, *Cell* **75**, 615 (1993).
- [5] G. Schatz and B. Dobberstein, *Science* **271**, 1519 (1996).
- [6] I. Szabò *et al.* *J. Biol. Chem.* **272**, 25275 (1997).
- [7] B. Hanss *et al.*, *PNAS USA* **95**, 1921 (1998).
- [8] J. J. Nakane, M. Akeson, A. Marziali, *J. Phys.: Cond. Mat.* **15**, R1365 (2003).
- [9] Yun-Long Tseng *et al.*, *Molecular Pharm.* **62**, 864 (2002).
- [10] J. M. Tsutsui *et al.*, *Cardiovasc. Ultrasound* **2**, 23 (2004).
- [11] J. Buchner, *FASEB J.* **10**, 10 (1996).
- [12] M. Magzoub, A. Pramanik and A. Gräslund, *Biochemistry* **44**, 14890 (2005).
- [13] G. J. L. Wuite *et al.*, *Nature* **404**, 103 (2000).
- [14] B. H. Leighton *et al.*, *J. Biol. Chem.* **281**, 29788 (2006).
- [15] Y. Kafri, D. K. Lubensky, D. R. Nelson, *Biophys. J.* **86**, 3373 (2004).
- [16] J. Kasianowicz *et al.*, *PNAS USA* **93**, 13770 (1996).
- [17] E. Henrickson *et al.*, *Phys. Rev. Lett.* **85**, 3057 (2000); A. Meller *et al.*, *Phys. Rev. Lett.* **86**, 3435 (2001); M. Akeson *et al.*, *Biophys. J.* **77**, 3227 (1999); A. Meller *et al.*, *PNAS USA* **97**, 1079 (2000); A. Meller and D. Branton, *Electrophoresis* **23**, 2583 (2002); A. J. Storm *et al.*, *Nanoletters* **5**, 1193 (2005).
- [18] I. Szabò *et al.*, *FASEB J.* **12**, 495 (1998); S. Horowka *et al.* *PNAS* **98**, 12996 (2001); S. Howorka, S. Cheley and H. Bayley, *Nature Biotechnol.* **19**, 636 (2001).
- [19] J. W. F. Robertson *et al.*, *Proc. Nat. Acad. Sci. USA* **104** 8207 (2007).
- [20] T. Ambjörnsson *et al.*, *J. Chem. Phys.* **117** 4063 (2002); W. Sung and P. J. Park, *Phys. Rev. Lett.* **77** 783 (1996); S. K. Lee and W. Sung, *Phys. Rev. E* **63** 012115 (2001); K. Lee and W. Sung, *Phys. Rev. E* **64** 041801 (2001); K. L. Sebastian and A. K. R. Paul, *Phys. Rev. E* **62** 927 (2000); K.K. Kumar and K. L. Sebastian, *Phys. Rev. E* **62** 7536 (2000); M. Muthukumar, *J. Chem. Phys.* **111** (1999); M. Muthukumar, *J. Chem. Phys.* **118** 5174 (2003); M. Muthukumar, *Phys. Rev. Lett.* **86** 3188 (2001); M. Muthukumar, *Electrophoresis* **23** 2697 (2002); C. Y. Kong and M. Muthukumar *J. Chem. Physics* **120** 3460 (2004); R. E. Boehm, *Macromolecules* **32** 7645 (1999); E. A. DiMarzio and J. J. Kasianowicz, *J. Chem. Phys.* **119** 6378 (2003); E. Slonkina and A. B. Kolomeisky, *J. Chem. Phys.* **118** 7112 (2003).
- [21] J. Mathé *et al.*, *Biophys. J.* **87**, 3205 (2004).
- [22] Y. Kantor and M. Kardar, *Phys. Rev. E* **69**, 021806 (2004).
- [23] I. Huopaniemi *et al.*, *Phys. Rev. E* **75**, 061912 (2007).
- [24] D. Panja, G. T. Barkema and R. C. Ball, e-print arxiv cond-mat/0703404.
- [25] P.-G. de Gennes, *Scaling Concepts in Polymer Physics*, Cornell University Press, Ithaca, 1979.
- [26] J. Klein Wolterink, G. T. Barkema and D. Panja, *Phys. Rev. Lett.* **96**, 208301 (2006).
- [27] D. Panja, G. T. Barkema and R. C. Ball, e-print arxiv cond-mat/0610671.
- [28] A. van Heukelum *et al.*, *Macromolecules* **36**, 6662 (2003); J. Klein Wolterink *et al.*, *Macromolecules* **38**, 2009 (2005); J. Klein Wolterink and G. T. Barkema, *Mol. Phys.* **103**, 3083 (2005).
- [29] There is however numerical evidence in Ref. (23) that the velocity of translocation is not constant in time (their Fig. 3).
- [30] Note that with $\phi(t)$ a constant, strictly speaking, the integral (9) does not converge. The divergence stems from the assumption that $\mu(t) \sim t^{-1/2}$ holds all the way to $t \rightarrow 0$. This is clearly not true as can be seen from Fig. 2(a), which provides the required cutoff for the convergence of the integral (9).